Received: 1 March 2017 | Revised: 23 May 2017 | Accepted: 23 May 2017

DOI: 10.1002/pat.4093

WILEY polymers advanced technologies

RESEARCH ARTICLE

# Self-reinforced polypropylene composites based on low-cost commercial woven and non-woven fabrics

José Luis Mijares[1] | Eliana Agaliotis[2] | Celina R. Bernal[2] | Mariana Mollo[3]

[1] National Commission of Atomic Energy (CNEA), Av. Gral. Paz 1499, 1650 San Martín, Argentina

[2] Institute of Technology in Polymers and Nanotechnology (ITPN), Faculty of Engineering, University of Buenos Aires, Av. Las Heras 2214, C1127AAR, Buenos Aires, Argentina

[3] Centre of Research and Development for the Plastics Industry (INTI-Plastics), Av. Gral. Paz 5445, B1650KNA, San Martín, Argentina

**Correspondence**
Mariana Mollo, Centre of Research and Development for the Plastics Industry (INTI-Plastics), Av. Gral. Paz 5445, B1650KNA, San Martín, Argentina
Email: mariana@inti.gob.ar

In the present paper, different self-reinforced polypropylene (PP) composites based on low-cost commercial woven (w) and non-woven (nw) fabrics were obtained. Hot compaction (HC) and film stacking (FS) followed by compression molding were used to prepared the composites. The fracture and failure behavior of the different materials was determined under different testing conditions through quasi-static uniaxial tensile tests, Izod impact experiments and by means of fracture mechanics tests on mode I double-edge deeply notched tensile specimens. In the case of the composite obtained by film stacking + compression molding (rPP/nw/w-FS) and the hot-compacted composite (nw/w-HC) containing simultaneously woven and non-woven fabrics, the acoustic emission technique was applied in situ in the tensile tests to determine their consolidation quality and to identify the failure mechanisms responsible for their fracture behavior. It was observed that both composites exhibited relatively similar high consolidation quality. However, the hot-compacted composite presented a more uniform distribution of failure mechanisms (debonding and fiber fracture) than the film-stacked composite. The hot-compacted composite containing both types of reinforcements exhibited the best combination of mechanical (tensile, impact, and fracture) properties. Therefore, this composite appeared as the most promising for structural applications among the different composites investigated.

KEYWORDS

fabrics, failure, fracture behavior, polypropylene, self-reinforced composites

## 1 | INTRODUCTION

Over the recent years, there has been an increasing interest toward self-reinforced composites. In these materials, the reinforcement is made of high strength highly oriented fibers or tapes while the matrix is a polymer of the same chemical nature but with a lower melting temperature. Self-reinforced composites compete with traditional composites in different applications depending on their performance/cost ratio. Among other advantages, the chemical compatibility of the components allows obtaining improved interfacial bonding between matrix and reinforcement. In addition, self-reinforced composites can be considered as environmentally friendly materials, being easily recyclable and having lower density in comparison with conventional composites. This latter advantage can be exploited to obtain light parts and structures.

A great number of papers have been published in the literature regarding the different aspects of many types of self-reinforced composites. Their thermal and mechanical behavior as well as their processing have been deeply investigated, as it has been comprehensively reviewed by Matabola et al[1] Karger-Kocsis and Bárány,[2] Gao et al,[3] and Kmetty et al.[4] However, at the time of writing to the authors knowledge, only a few of these investigations have focused on self-reinforced composites with non-woven fabrics or similar reinforcement geometries, and no works have been published regarding the simultaneous application of woven and non-woven fabrics.

One of the most widely used methods to produce self-reinforced composites is hot compaction (HC). It has the advantage that the matrix phase is obtained around each fiber by melting and recrystallization, without the need of any other material for the matrix phase. Thus, remarkable interfacial bonding between the oriented phase acting as reinforcement and the melted and recrystallized phase acting as matrix can be achieved.[5,6] Among other methods to obtain self-reinforced polymer composites are consolidation of coextrusion tapes or film stacking (FS). The advantages of the FS method are a wide processing window, no expensive preproduction, and the possibility to use any kind of polymer.[7,8]

In the present paper, different self-reinforced PP composites based on commercial woven and non-woven fabrics were prepared

  

by HC or by FS followed by compression molding. The aim was to obtain a material with a good combination of mechanical properties from the use of low-cost commercial reinforcements. The fracture and failure behavior of these composites was determined under different testing conditions. This behavior was characterized through quasi-static uniaxial tensile tests, Izod impact experiments, and by means of fracture mechanics through quasi-static tensile fracture tests on mode I double-edge deeply notched tensile specimens. In addition, the acoustic emission technique was applied in situ in the tensile tests to determine the consolidation quality of the different composites and to identify the failure mechanisms responsible for the materials fracture behavior.

The self-reinforced composites developed in this work took advantage of the use of low-cost commercial woven and non-woven PP fabrics, as it was mentioned before. In the case of the film-stacked self-reinforced composites, a relatively wide processing window was obtained from the difference in melting temperatures between the higher melting temperature stretched PP homopolymer[8] that composed the fibers of both types of fabrics and the commercial random PP copolymer (rPP) with lower melting temperature[9] used as the matrix. This was based on the original idea of Alcock et al[10] to increase the processing window in self-reinforced PP.

## 2 | MATERIALS AND METHODS

### 2.1 | Methods

#### 2.1.1 | Chemical characterization

To identify the chemical nature of the different materials, Fourier transform infrared spectroscopy (FTIR) was used. Transmission infrared absorption spectra were recorded by using an FTIR Nicolet 5700-Omnic spectrometer.

#### 2.1.2 | Morphology

The materials morphological characterization was performed by means of scanning electron microscopy (SEM) in an SEM Quanta FEG 250. Cryogenic fracture surfaces were obtained at liquid nitrogen temperature. Samples were sputtered coated with a thin layer of gold before SEM observations.

#### 2.1.3 | Thermal characterization

Thermal analysis was carried out in a differential scanning calorimeter (DSC) Mettler 822e/500/1473. Dynamic analysis was performed by heating scan from 30 °C to 200 °C at a rate of 5 °C/min. For those composite samples containing woven and non-woven fabrics as reinforcement, a first heating scan was performed at 2 °C/min to observe in detail melting endotherms in the zone of the melting of the fibers.

The degree of crystallinity was determined by using the following equation:

$$\%_{cr} = \Delta H_f \, x \, 100/\Delta H_0 \quad (1)$$

where $\Delta H_f$ is the experimental value of the melting energy and $\Delta H_0$ is the melting energy or heat for the 100% crystalline PP. This is a theoretical value taken as 190 J/g in this work.[11]

#### 2.1.4 | Mechanical characterization

Uniaxial tensile tests were carried out on type IV (ASTM D638) dumbbell samples cut out from the matrix films and the composite plaques in an INSTRON dynamometer 5569 at 50 mm/min. Stress-strain curves were obtained from these tests, and tensile parameter values (Young's modulus, tensile strength, and strain at break) were determined from these curves.

To characterize the non-woven fabric under uniaxial tension, rectangular coupons having 15 mm in width, 165 mm in length, and 0.4 mm in thickness were also tested under uniaxial tension at 50 mm/min. The woven fabric had been previously characterized in another investigation.[12]

Izod impact experiments were also carried out on rectangular V-notched composite samples by following ASTM D256 standard recommendations in a CSI (CS-137D-177) Izod pendulum.

In addition, the acoustic emission technique (AE) was also applied in situ in the tensile tests to determine the consolidation quality of the different composites and to identify the failure mechanisms responsible for their fracture behavior. A VN525 Single channel Time Domain AE Analyzer in the frequency range of 100… 600 kHz with logarithmic amplification was used. The threshold was set as 40 $dB_{AE}$, and the reference amplitude was 4–5 V. The piezoelectric sensor was set in the center of the sample. To enhance wave propagation through the different media, a thin layer of silicon grease was applied between the specimen surface and the AE sensor. The maximum amplitude and the cumulative number of events were recorded.

Quasi-static fracture characterization was carried out on mode I double-edge deeply notched tensile specimens cut out from the composite plaques (nominal width $W$ was 23 mm and nominal length $S$ was 50 mm), at a cross-head speed of 10 mm/min. Sharp notches were introduced by scalpel-sliding a fresh razor blade into a machined slot. Crack/width ratio ($a/W$) was maintained at 0.5.

Critical stress intensity factor ($K_{IQ}$) at 5% non-linearity was obtained as described previously by Pettarin et al[13] and used here to characterize the material resistance to crack initiation.

Critical energy release rate values at propagation ($G_{CP}$) were also determined from the total area under the load–displacement curve ($U_{tot}$), as follows[14]:

$$G_{CP} = U_{tot}/B\,(W-a) \quad (2)$$

All mechanical tests were carried out at room temperature.

### 2.2 | Matrix and reinforcements

Films (nominal thickness = 0.2 mm) of a commercial random PP copolymer 3240 NC (rPP) (Petroquimica Cuyo SAIC, Mendoza, Argentina) were obtained by cast extrusion using a single screw Killion KL-10 with a flat die and a chill roll system. A standard 25 mm screw with an L/D ratio of 24:1 was used. Processing parameters were controlled as follows:

- Zone 1: 165 °C
- Zone 2: 165 °C
- Zone 3: 165 °C

- Die: 157 °C
- Outlet temperature: 170 °C
- Speed: 60 rpm

The obtained films were used as the matrix of those composites obtained by FS.

FTIR spectrum for the random copolymer corresponds to typical PP spectrum.[15] Other bands that can be assigned to polymerized ethylene from the copolymerization process were also observed.

Films melting temperature was 151 °C and degree of crystallinity was 36%. These thermal parameters were similar to the values obtained for pristine rPP, indicating that the material was not subjected to significant molecular orientation during film extrusion.

Commercial non-woven (nw) and woven (w) fabrics were used as reinforcement.

The non-woven fabric (55 g/m$^2$) was kindly provided by PGI, Argentina. This fabric, made up of non-woven PP homopolymer fibers, was composed of 3 layers. The external layers were made of continuous PP homopolymer extruded fibers (21 μm average diameter). The intermediate layers were made of short fibers with smaller diameter (9 μm average diameter) (Figure 1A). Melting temperature of non-woven fabric was 172 °C, determined by DSC. The degree of crystallinity was 47% (first heating scan). Consolidation of the fabric was attained in a calander by thermo-welding. The orthorombic points of the thermo-welded zones are clearly observed in Figure 1B.

A commercial woven PP fabric composed of highly stretched PP yarns, kindly provided by Politejidos S.R.L., Argentina (190 g/m$^2$) (Figure 2). was also used as reinforcement. In this fabric, a range of melting temperature between 173 °C and 178 °C was observed[12] This result indicated that this fabric presented zones with different melting temperatures, as a result of the different stretching levels obtained during processing.

The FTIR spectra for the non-woven and woven PP fabrics were in agreement with reference spectra for PP homopolymer reported in the literature.[15] However, for the woven fabric, bands at 714, 876 and 1797 cm$^{-1}$ were also observed. These bands were attributed to the presence of inorganic carbonates such as calcium carbonate.

## 2.3 | Self-reinforced composites

Three types of self-reinforced composites were obtained in this work. The materials and processing techniques used are summarized as follows:

- **rPP/nw-FS**: extruded films of rPP as the matrix and commercial non-woven fabric (nw) as reinforcement, obtained by FS followed by compression molding.
- **rPP/nw/w-FS**: extruded films of rPP as the matrix and intercalated non-woven (nw) and woven (w) fabrics as reinforcement, obtained by FS followed by compression molding.
- **nw/w-HC**: intercalated non-woven and woven fabrics, obtained by HC.

All of the composites were obtained with a hydraulic press (Smaniotto AMS 160/39). Cooling was performed by circulating water from the processing temperature to room temperature at the same cooling rate to impart the same thermal history to all the samples.

### 2.3.1 | Self-reinforced composites obtained by FS

Self-reinforced composites were obtained by FS followed by compression molding by using the extruded films of rPP as the matrix and the commercial non-woven (nw) and woven (w) fabrics as reinforcement. Consolidation of the film-stacked composites was obtained by compression molding in a hydraulic press Smaniotto AMS 160/39, with a maximum capacity of 40 ton.

For the **rPP/nw-FS** composite, a pressure of 7 MPa was selected based on previous investigations on similar composites.[16,17] Compression molding temperature was determined by analyzing DSC thermograms of rPP (matrix) and nw fabric (reinforcement). To obtain good adhesion between matrix and reinforcement, processing temperature was set at 155 °C. Based on calorimetric data, at that temperature, only a small part of the surface of the fibers was expected to be melted. The number of alternating layers of matrix and reinforcement was 6 and 5, respectively. Further increase in the number of layers

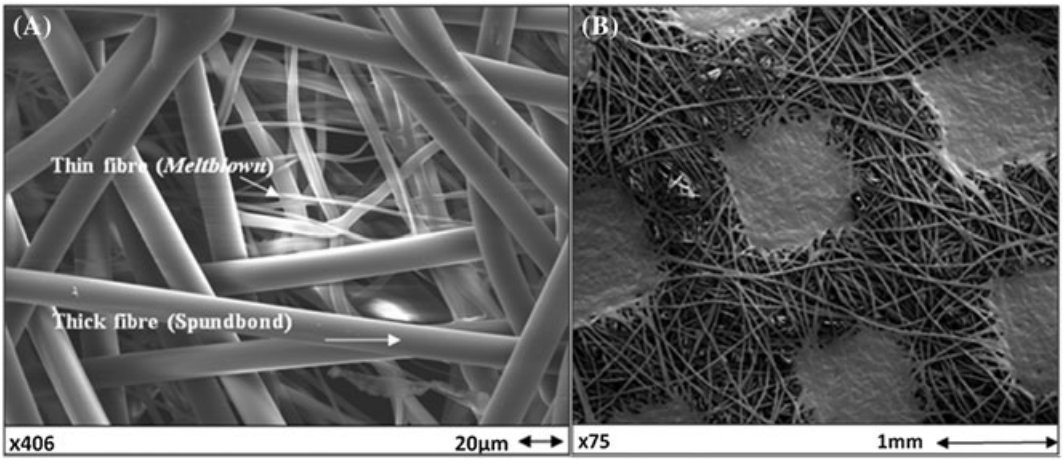


**FIGURE 1** SEM micrographs of the commercial non-woven fabric used as reinforcement. (a) View of the non-woven fibers; (b) orthorombic points of the thermowelded zones

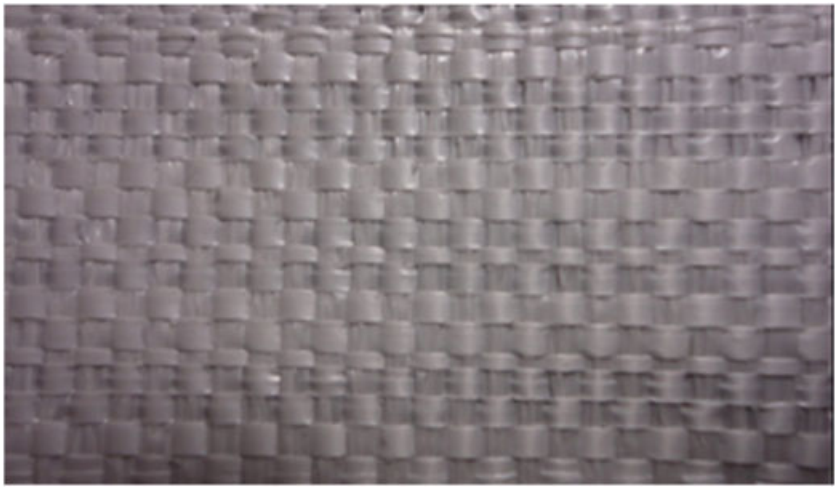

**FIGURE 2** Commercial woven PP fabric used as reinforcement [Colour figure can be viewed at wileyonlinelibrary.com]

led to composite delamination because of the lack of melting of intermediate layers.

Once the selected molding temperature had been reached, alternating layers of rPP and nw were set in the hydraulic press between 2 Teflon films. A time interval ($t_1$) was kept without any pressure to enhance matrix melting. Then a second time interval ($t_2$) was maintained allowing the melted matrix to interpenetrate among the fibers and hence to obtain good adhesion between phases. Finally, the material was cooled down to room temperature by circulating water within the press plates.

Different molding times were used, taking into account previous works reported in the literature on similar composites.[7,17] The optimal selected times for **rPP/nw-FS** were $t_1$ 30 s (without pressure) and $t_2$ 30 s (with pressure).

The use of a short molding time of 30 s was chosen to melt only a small portion of the surface of the fibers. The mass percentage of initial reinforcement set in the mold was determined, taking into account the number and the mass of the rPP and nw layers used. A value of around of 16% was found for the **rPP/nw-FS** composite.

For the **rPP/nw/w-FS** composite, time and temperature parameters were varied to determine optimal processing conditions. The best properties were observed at the same conditions than those used for the **rPP/nw-FS** composite. Because of the presence of the woven fabric, an initial pressure of 2 MPa was used.[18] The aim of this initial pressure was to avoid fiber shrinking due to heat. This initial pressure was maintained during $t_1$. Then it was increased up to 7 MPa. The higher pressure was kept for $t_2$, and then the material was cooled down to room temperature by circulating water within the press plates. Figure 3 shows a schematic diagram of the layer structure for both composites.

### 2.3.2 | Self-reinforced composite obtained by HC

Intercalated non-woven and woven fabrics were processed by HC to obtain another self-reinforced PP composite (**nw/w-HC**). In this composite, melting of the external surface of the fibers constituted the matrix.

To determine adequate processing conditions (temperature, time, and pressure) for the self-reinforced composite obtained by HC, preliminary investigations on self-reinforced PP composites based on woven fabrics were taken into account.[18]

Once the press temperature had reached 100 °C, layers of reinforcement were set within the press plates under a pressure of 2 MPa, and when molding temperature had been attained,

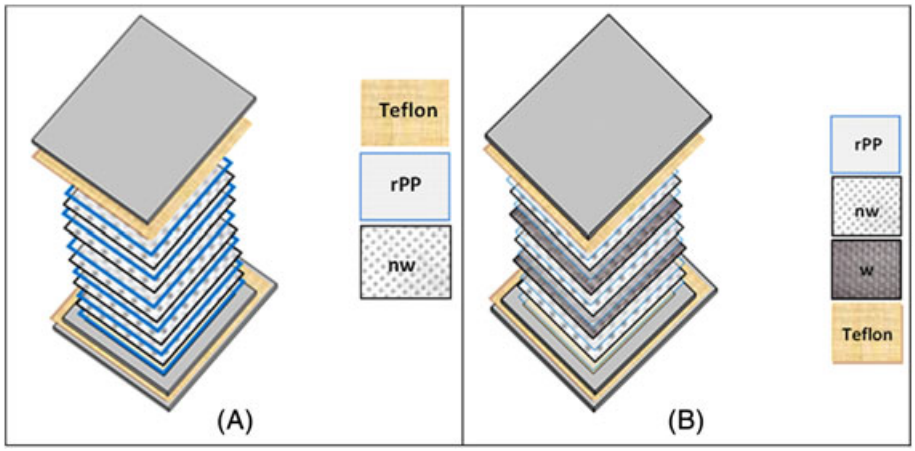


**FIGURE 3** Schematic diagram of the layer structure of the composites: (a) **rPP/nw-FS**; (b) **rPP/nw/w-FS** [Colour figure can be viewed at wileyonlinelibrary.com]

temperature was kept during 600 s ($t_1$). Then a pressure of 10 MPa was maintained for 30 s ($t_2$), and the material was cooled down to 60 °C under pressure. At this temperature, the plaque was taken out of the press and slowly cooled down to room temperature under a slight pressure.

With the aim to obtain plaques with thickness similar to film-stacked composites plaques, 5 layers of woven fabric and 4 layers of non-woven fabric were used. Based on previous results on hot-compacted self-reinforced PP composites containing woven fabrics (optimal processing temperature between 165 °C and 170 °C), a molding temperature of 165 °C was chosen in this case. A higher increase of temperature would have produced excessive fiber melting and/or relaxation with the subsequent detrimental effect on the composite mechanical properties.

## 3 | RESULTS AND DISCUSSION

### 3.1 | Morphology

Figure 4 presents an SEM micrograph of the cryogenic fracture surface of the **rPP/nw-FS** composite. The presence of 5 layers of fabric is clearly observed in this figure, thus indicating that reinforcement structure was maintained and it was only partially melted during processing.

Figure 5 shows an SEM micrograph obtained for an **rPP/nw/w-FS** composite sample. The external layer, which corresponds to the rPP layer, as well as the woven fabric layer can be clearly observed in Figure 5A. A closer view of the same micrograph (Figure 5B) shows some fibers from the non-woven fabric. Average diameter value for these fibers was found to be 17 μm, which is lower than the 21-μm diameter value of the original continuous fibers (Figure 1B). In this case, the woven fabric structure was preserved during processing, whereas the non-woven fabric was mostly melted. This diameter reduction can be attributed to the melting of the external layer of the fibers during processing. The surrounding material of the fibers, which has a completely different aspect respect to the woven fabric, would correspond to the melted non-woven fabric and rPP layers. A few fibers from the non-woven fabric are only observed. This could be due to the fact that most of these fibers were melted during processing. Problems associated with cryogenic fracture could also have contributed to the difficulty in fibers observation.

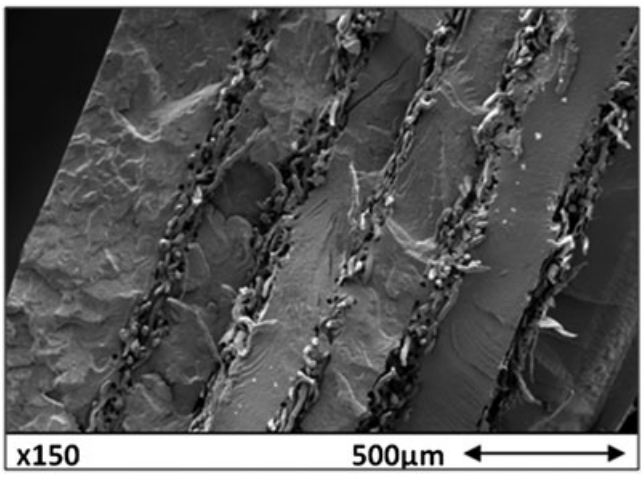


**FIGURE 4** SEM micrograph of the cryogenic fracture surface of the **rPP/nw-FS** composite

Figure 6A presents an SEM micrograph obtained from the cryofractured surface of a **nw/w-HC** composite sample. In this figure, the presence of the woven fabric is evident. A closer view of the same micrograph (Figure 6B) shows small aligned voids. These voids correspond to the fibers from the non-woven fabric, which were pulled out during fracture at liquid nitrogen temperature. The diameter of these voids is 18 μm, in agreement with the value observed for the fibers from the non-woven fabric in the **rPP/nw/w-FS** composite (Figure 5B). In addition, the zone of the voids presents a particular appearance different from the woven PP fabric as that zone is composed by the melting of the non-woven fibers. However, similar to what happened in the **rPP/nw/w-FS** composite, the fibers could be not clearly distinguished. As it was noted before, for the composites obtained by FS, melting of the fibers from the non-woven fabric during processing or problems associated with cryogenic fracture could be responsible for the absence of these fibers in SEM micrographs. Once again, the woven fabric was the unique reinforcement mainly preserved during processing of composites containing both types of fabrics.

### 3.2 | Thermal analysis

Melting temperatures for the different composites investigated, obtained by DSC, are summarized in Table 1. Thermal values for neat matrix and reinforcements are also included in this table for comparison. Corresponding DSC thermograms are shown in Figure 7.

For both composites obtained by film stacking (**rPP/nw-FS** and **rPP/nw/w-FS** composites), 3 melting endotherms were observed. The first melting, $T_{m1}$, corresponds to the melting of the rPP matrix. The endotherm found at $T_{m3}$ corresponds to the melting of the PP homopolymer fibers. The presence of the melting at $T_{m2}$ indicates that a small portion of the external surface of the fibers melted and crystallized during cooling in the mold, eliminating the orientation and decreasing the PP melting temperature. This melting of the external layer was expected to improve interfacial adhesion between matrix and reinforcement.

For the **rPP/nw-FS** composite, the existence of the endotherm at 170 °C ($T_{m3}$) confirmed the presence of non-woven fibers in agreement with SEM observations.

The endotherm observed at 168 °C ($T_{m2}$) for the **rPP/nw/w-FS** composite corresponds to the melting of the external surface of the fibers. Because of the woven and non-woven fibers melted in a similar temperature range, it was not possible to identify which fiber had melted.

For the **nw/w-HC** composite, on the other hand, 2 endotherms were observed: at 169 °C ($T_{m2}$) and at 176 °C ($T_{m3}$). The latter corresponds to the melting of the fibers. Melting of the external surface of the fibers during processing led to the endotherm at 169 °C, indicating the presence of unoriented PP homopolymer.

Composites reinforcement contents before and after processing are presented in Table 2. Values before processing were determined from the initial weight of the woven and non-woven layers used to

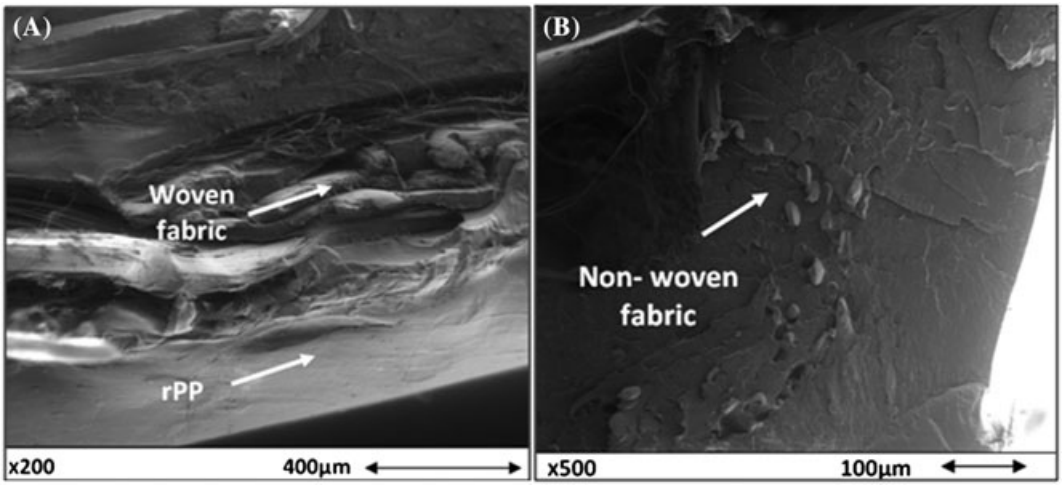


**FIGURE 5** SEM micrographs for a **rPP/nw/w-FS** composite sample at different magnifications, (a) ×200 and (b) ×500

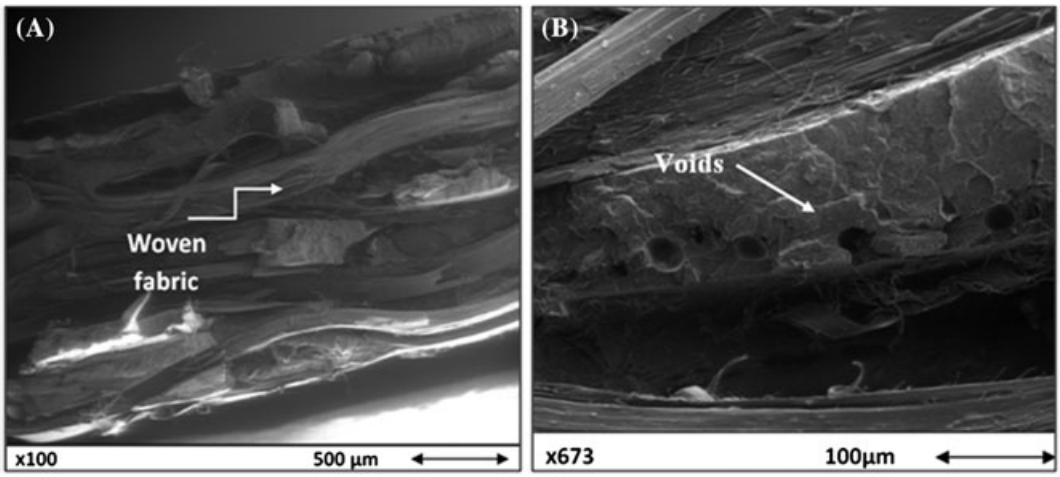


**FIGURE 6** SEM micrograph of a **nw/w-HC** composite sample. (a) Lower magnification and (b) higher magnification

**TABLE 1** Melting temperatures for the different composites investigated.

| Sample | $T_{m1}$, °C | $T_{m2}$, °C | $T_{m3}$, °C |
|---|---|---|---|
| **rPP** | 151 | – | – |
| **nw** | – | – | 172 |
| **w** | – | – | 173–178 |
| **rPP/nw-FS** | 154 | 164 | 170 |
| **rPP/nw/w-FS** | 151 | 168 | 174 |
| **nw/w-HC** | – | 169 | 176 |

prepare each type of composites while values after processing were obtained from image analysis of optical micrographs with the help of an image processing commercial software (ImageJ).

For the **rPP/nw-FS** composite, reinforcement content before and after processing was rather similar. However, it was confirmed by DSC that part of the fibers from the non-woven fabric were melted (melting endotherm at $T_{m2}$) during processing. The percentage of fibers incorporated in this case is low because of the low weight of nw layers required for the FS process. Hence, the amount of melted material (confirmed by DSC) is not enough to be detected by image analysis.

For the **rPP/nw/w-FS** and for the **nw/w-HC** composites, on the other hand, the content of both types of fibers (from woven and non-woven fabrics) and the content of woven fibers decreased, respectively, as a result of their melting and subsequent recrystallization to take part of the matrix, in agreement with DSC results.

## 3.3 | Uniaxial tensile behavior

Tensile parameter values for neat matrix and reinforcements were obtained as reference values. In the case of the rPP copolymer matrix, these values were similar to those reported by the producer (Table 3).

To determine the maximum stress value for the non-woven fabric, actual stress values were determined by taking into account that the fabric was composed of fibers and voids instead of being a continuous material. This was made calculating actual stress values as follows:

$$\sigma_{real} = \sigma \, x \, \delta_{PPh}/\delta_{PPnw} \quad (3)$$

where $\delta_{PPh}$ is the density of the PP homopolymer and $\delta_{PPnw}$ is the density of the non-woven PP fabric.

The density of the PP homopolymer that constituted the fibers of the non-woven fabric was calculated based on the degree of

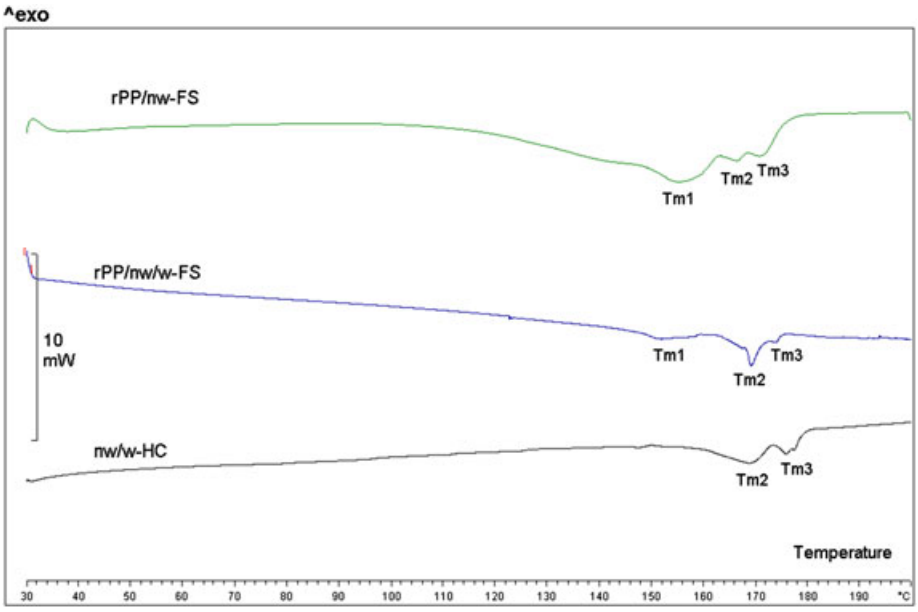


**FIGURE 7** DSC thermograms for the different composites investigated [Colour figure can be viewed at wileyonlinelibrary.com]

**TABLE 2** Reinforcement content before and after processing

| Sample | Before processing | After processing |
|---|---|---|
| **rPP/nw-FS** | 16% nw | 18% nw |
| **rPP/nw/w-FS** | 8% nw–22% w | 6% nw–12.5% w |
| **nw/w-HC** | 18% nw–82% w | 23.7% matrix (melted w and nw)–76.3% w (nw could not be measured) |

**TABLE 3** Mechanical parameter values along with their deviations (between brackets)

| Sample | Young's modulus, MPa | Tensile strength, MPa | Strain at break, % | Izod impact strength, kJ/m$^2$ |
|---|---|---|---|---|
| **rPP** | 1040 (22) | 27 (1) | 15 (2) | 12 (2) |
| **rPP/nw-FS** | 1275 (91) | 31 (1) | 11 (5) | 13 (3) |
| **rPP/nw/w-FS** | 1167 (43) | 52 (5) | 20 (1) | 41 (10) |
| **nw/w-HC** | 1410 (108) | 54 (13) | 15 (2) | 59 (19) |

crystallinity (47%), and assuming the density of the amorphous phase, $\delta_a$ = 0.850 g/cm$^3$ and the density of crystal, $\delta_{cr}$ = 0.940 g/cm$^3$.[19] The density value for the PP homopolymer of the fibers (0.890 g/cm$^3$) was calculated using a weighted average formula.

The density of the non-woven PP fabric (0.138 g/cm$^3$) was obtained by taking into account the weight fabric (55 g/m$^2$) and the thickness (0.04 cm). In accordance with equation 3, the corrected maximum stress was 48 MPa.

The results of the mechanical characterization of the woven PP fabric have been previously reported in another investigation.[12] They are also included in this work only for comparison: maximum longitudinal and transversal stress values were 153.4 MPa and 117.4 MPa, respectively.

The **rPP/nw-FS** composite exhibited limited ductility in tensile tests, with neither stress whitening nor significant necking. Stress-strain curves (not shown) displayed non-linear behavior until maximum load followed by a sharp drop of load until zero near that point. Furthermore, because the non-woven fabric is composed of fibers not aligned in the tensile direction, only marginal improvements in tensile properties (stiffness and strength) were found for this composite respect to the matrix (Table 3).

The **rPP/nw/w-FS** composite also presented non-linear tensile behavior with an abrupt fall of load at final fracture before the maximum. No significant differences in Young's modulus or strain at break values were found respect to rPP (Table 3). However, an important increase of strength (92%) was observed for this composite.

The best tensile properties were presented by the **nw/w-HC** composite: improved stiffness was found respect to film-stacked composites while tensile strength was similar to that of the **rPP/nw/w-FS** composite obtained by FS with intercalated non-woven and woven PP fabrics which exhibited the highest strength between both film-stacked composites.

## 3.4 | IZOD impact strength

For the **rPP/nw-FS** composite, no significant changes respect to the rPP matrix were observed in Izod strength values. However, the incorporation of the woven fabric as reinforcement led to a significant

improvement (240%) of impact strength for the **r/nw/w-FS** composite. In addition, the best impact behavior was exhibited by the **nw/w-HC** composite (Table 3) with a 6 times increase of Izod strength respect to rPP.

From the above results, it seems that the presence of the woven fabric is essential to obtain composites with improved mechanical properties.

In addition, morphological observations by SEM and thermal analysis showed that the woven fabric was practically the only reinforcement preserved during processing in the case of the composites containing both types of fabrics, irrespective of the processing method used. Hence, the non-woven fabric would have mainly acted as an additional source of matrix material leading to a decrease in the actual reinforcement volume fraction similarly to what happened with the interleaved films used by Foster et al[20] in hot-compacted composites.

## 3.5 | Fracture behavior

As the composite containing only non-woven fabric as reinforcement (**rPP/nw-FS**) did not lead to a significant improvement of tensile and Izod properties respect to neat matrix, this composite was not considered in the subsequent analysis of fracture and failure behavior.

All samples of **rPP/nw/w-FS** and **nw/w/HC** composites exhibited fracture behavior with ductile instability,[21], ie, non-linear load–displacement behavior with some amount of slow crack growth preceding unstable fracture (Figure 8). At initial steps, stable crack propagation existed and, at a certain point in the load–displacement curve, propagation mode became unstable and a sharp load drop at the point of fracture was observed.

According to linear elastic fracture mechanics,[22] for valid plane strain fracture toughness determinations, linear-elastic behavior up to the point of fracture and plane strain conditions are simultaneous requirements. Although they were not satisfied in our experiments, the initiation parameter values still reflect a critical state for crack initiation.[23] Hence, critical stress intensity factor ($K_{IQ}$) values at initiation were used in this work to compare the fracture initiation behavior of our composites. Critical energy release rate values at propagation ($G_{CP}$) were also determined and they were adopted as a measure of the resistance to crack propagation. Both fracture parameter values are presented in Table 3 along with their deviations.

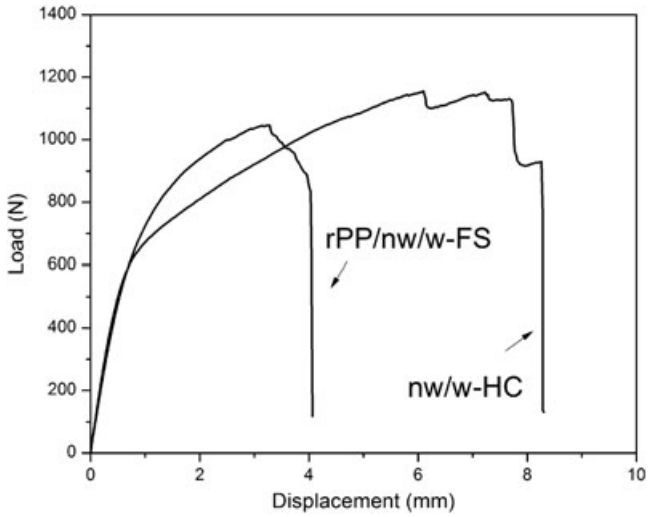


**FIGURE 8** Typical load–displacement curves obtained in fracture tests for the **rPP/nw/w-FS** and **nw/w-HC** composites

Although critical initiation values were similar for both composites investigated, a significantly higher critical propagation value was observed for the composite obtained by HC, indicating that more energy was dissipated during crack growth in this material.

It can be also observed in Figure 8 that the **rPP/nw/w-FS** and **nw/w-HC** composites samples exhibited a stepwise drop of load from the maximum (pop-ins), before the instability point, suggesting the presence of a growing mechanism of successive stops and accelerations of crack (stick–slip mechanism). The failure was mainly due to fiber fracture, delamination and tape pullout of the woven fabric and the load suddenly dropped at the point of fracture, leaving a remaining load due to the longest fibers that were still sustaining load. However, the hot-compacted composite (**nw/w-HC**) displayed higher load steps and more significant lateral stress whitening. This evidenced higher damage in this composite, and consequently, more energy was absorbed in this case during crack propagation leading to a significantly higher critical energy release rate propagation value (Table 4).

## 3.6 | Failure behavior

Finally, acoustic emission analysis was also used to identify the main failure mechanisms operative in the **rPP/nw/w-FS** and **nw/w-HC** composites such as fiber fracture, delamination and tape pullout of the woven fabric, as mentioned before. These were also correlated with the materials fracture behavior.

With the aim to compare the curves of cumulative number of events *versus* deformation, which can be used to evaluate the consolidation quality of the composites, the acoustic emission events were recorded until fracture during tensile tests. The failure mechanisms operative in the self-reinforced composites were also analyzed from the relative number of events *versus* maximum acoustic emission amplitude values as explained elsewhere.[24] Figures 9 and 10 present the obtained results for the **rPP/nw/w-FS** and **nw/w-HC** composites, respectively.

As it can be observed in Figures 9A and 10A, both self-reinforced composites investigated presented only a few AE events at the beginning of the test and the number of events sharply increased near final fracture. In addition, the total number of events had nearly the same low value (around 65 events). It has been previously reported[24] that composite materials with higher consolidation quality exhibit acoustic emission events lately near final fracture and the total number of

**TABLE 4** Critical initiation and propagation values for the composites containing both types of fabrics (standard deviation between brackets)

| Sample | $K_{IQ}$, MPa.m$^{1/2}$ | $G_{CP}$, kJ/m$^2$ |
|---|---|---|
| **rPP/nw/w-FS** | 2.6 (0.4) | 144.4 (31.0) |
| **nw/w-HC** | 2.7 (0.2) | 240.7 (85.3) |

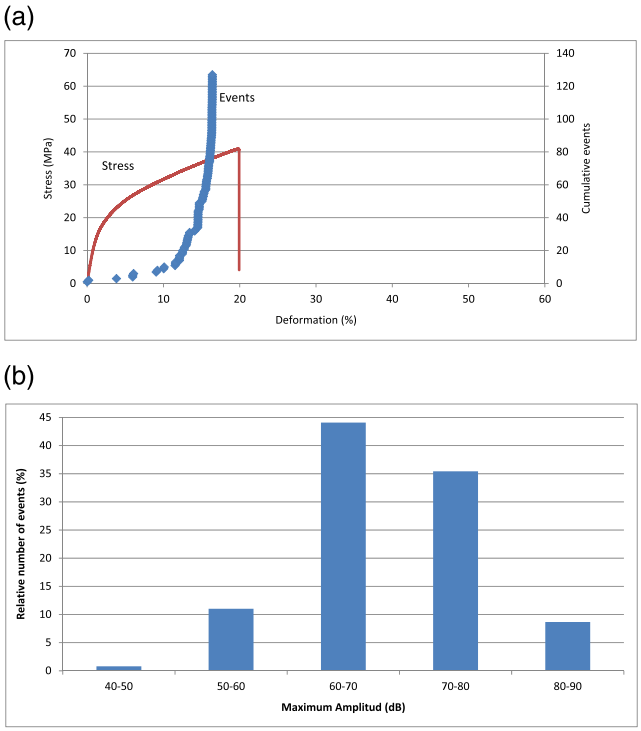


**FIGURE 9** Acoustic emission results for the **rPP/nw/w-FS** composite. (a) Cumulative number of events vs. deformation. (b) Relative number of events vs. maximum amplitude [Colour figure can be viewed at wileyonlinelibrary.com]

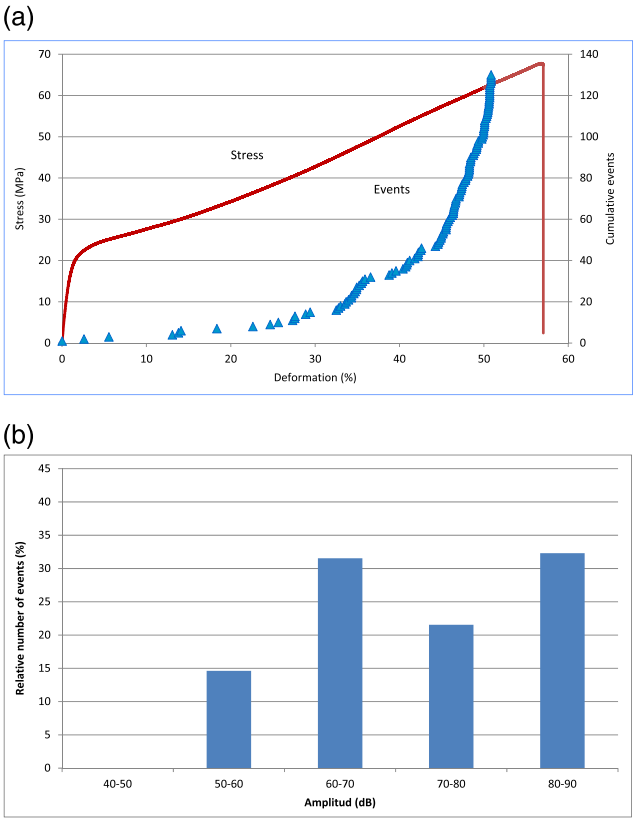


**FIGURE 10** Acoustic emission results for the **nw/w-HC** composite. (a) Cumulative number of events vs. deformation. (b) Relative number of events vs. maximum amplitude [Colour figure can be viewed at wileyonlinelibrary.com]

events is lower than composites with poorer consolidation. This result suggested that both **rPP/nw/w-FS** and **nw/w-HC** composites exhibited similar relatively high consolidation quality.

In addition, the analysis of the relative number of events *versus* maximum acoustic emission amplitude values (Figures 9B and 10B) showed different failure patterns for both composites. While for the **rPP/nw/w-FS** composite medium amplitude events such as debonding and delamination were mostly dominant (44% of 60–70 dB and 35% of 70–80 dB), a much more uniform pattern was found for the **nw/w-HC** composite. Moreover, for this composite, a significantly higher relative number of events of high amplitude (80–90 dB) was detected. Other results on self-reinforced composites with woven fabrics[25] have shown that the events of 40–50 dB can be assigned to the movement of the threads in the woven fabric. In addition, AE analysis of the non-woven fabric was also developed in this investigation but only a few number of events, which can be neglected, were observed. Hence, low amplitude events in our self-reinforced composites were only attributed to the movement of the woven reinforcement which induced its debonding from the matrix. Higher amplitude acoustic emission events, on the other hand, were mostly attributed to fiber fracture. Therefore, the **nw/w-HC** composite, clearly presented more balanced failure mechanisms which contributed to the higher mechanical performance exhibited by this composite (higher tensile strength and impact and fracture propagation resistance).

The more uniform pattern of relative number of events *versus* maximum AE amplitude observed in the hot-compacted composite, with respect to the composite obtained by FS, would also suggest that the former had a higher content of reinforcement which would confirm morphological observations.

## 4 | CONCLUSIONS

Self-reinforced PP composites based on low-cost commercial woven and non-woven fabrics were obtained by FS followed by compression molding and by HC. Their fracture and failure behavior was characterized by means of uniaxial tensile, Izod impact and fracture tests.

Although the incorporation of non-woven PP fabrics into the rPP matrix did not show any improvement in the mechanical properties, a significant increase in tensile strength and Izod impact strength was observed with the combination of non-woven and woven PP fabrics.

The HC technique seems to be better than FS followed by compression molding to obtain self-reinforced composites based on low-cost commercial woven and non-woven PP fabrics with a good combination of mechanical (tensile, impact and fracture) properties.

The acoustic emission technique applied in situ in the tensile tests allowed to compare the consolidation quality of the different composites and also to identify the failure mechanisms responsible for their fracture behavior. It was observed that both **rPP/nw/w-FS** and **nw/w-HC** composites exhibited relatively similar high consolidation quality. However, the hot-compacted composite presented a more balanced combination of debonding and fiber fracture than the

film-stacked composite containing both types of fabrics probably due to the lower content of reinforcement in the latter.

The results of this research suggest that the composite containing simultaneously woven and non-woven fabrics obtained by HC (nw/w-HC) is the most promising composite for structural applications among the different composites investigated.

## REFERENCES


1. Matabola KP, De Vries AR, Moolman FS, Luyt AS. *J Mater Sci*. 2009;44:6213-6222.
2. Karger-Kocsis J, Bárány T. *Compos Sci Technol*. 2014;92:77-94.
3. Gao C, Yua L, Liu H, Chen L. *Prog Polym Sci*. 2012;37:767-780.
4. Kmetty A, Barany T, Karger-Kocsis J. *Prog Polym Sci*. 2010;35:1288-1310.
5. Ward IM, Hine PJ. *Polymer*. 2004;45:1413-1427.
6. Foster RJ, Hine PJ, Ward IM. *Polymer*. 2016;91:156-161.
7. A. Izer, Development and investigation of self-reinforced PP composites based on the polimorphism of PP, PhD Thesis, Budapest University of Technology and Economics, 2010.
8. Chen JC, Wu CM, Pu FC, Chiu CH. *eXPRESS Polymer Letters*. 2011;5:228-237.
9. Morgan LM, Weager BM, Hare CM, Bishop GR. Self reinforced polymer composites: Coming of age, in Proceeding of the 17th International Conference on Composite Materials, Edimburgh, UK, ID12:15, 2009.
10. Alcock B, Cabrera NO, Barkoula N-M, Spoelstra AB, Loos J, Peijs T. *Composites Part A*. 2007;38:147-161.
11. Mettler Toledo. *Collected Applications: Thermal Analysis Thermoplastics*. Switzerland: Mettler; 1997.
12. Lucchetta MC, Morales Arias JP, Mollo M, Bernal C. *Polym Adv Technol*. 2016;27:1072-1081.
13. Pettarin V, Brun F, Viana JC, Pouzada A, Frontini PM. *Compos. Sci. Technol.* 2013;74:28-36.
14. Adams MJ, Williams D, Williams JG. *J Mater Sci*. 1989;24:1772-1776.
15. Hummel DO. *Atlas of Polymer and Plastics Analysis*. Munich, Vienna, Weinheim, New York: Hanser Publishers; 1991.
16. Bárány T, Izer A, Karger-Kocsis J. *Polym Test*. 2009;28:176-182.
17. Izer A, Bárány T, Varga J. *Compos. Sci. Technol.* 2009;69:2185-2192.
18. Bernal C, Lucchetta MC, Méndez R, Mijares JL, Mollo M. *31th Danubia-Adria Symposium*. September, Germany: Kempten University; 2014.
19. Pasquini N. *Polypropylene Handbook*. Munich, Hanser Gardner Publications, Cincinatti: Hanser Publishers; 2005.
20. Foster RJ, Hine PJ, Ward IM. *Polymer*. 2010;51:1140-1146.
21. Martinez AB, Gamez-Perez J, Sanchez-Soto M, Velasco JI, Santana OO, Ll Maspoch M. Engin. *Failure Anal*. 2009;16:2604-2617.
22. Williams JG. *Fracture Mechanics of Polymers*. London, UK: Ellis Horwood Limited; 1984.
23. Gensler R, Plummer CJG, Grein C, Kausch HH. *Polymer*. 2000;41:3809-3819.
24. Romhány G, Bárány T, Czigány T, Karger-Kocsis J. *Polym. Adv. Technol.* 2007;18:90-96.
25. Hine PJ, Ward IM, Matty MIA, Olley RH, Bassett DC. *J Mater Sci*. 2000;35:5091-5099.


**How to cite this article:** Mijares JL, Agaliotis E, Bernal CR, Mollo M. Self-reinforced polypropylene composites based on low-cost commercial woven and non-woven fabrics. *Polym Adv Technol*. 2017. https://doi.org/10.1002/pat.4093